

Detection of Patient Motion During Tomographic Myocardial Perfusion Imaging

Jeffrey A. Cooper, Paul H. Neumann and Brian K. McCandless

Department of Radiology, Albany Medical College, Albany, New York

We compared the effectiveness of four methods for detecting patient motion during tomographic myocardial perfusion imaging: visual inspection of a cine of the raw data, cross-correlation, diverging squares and a new method called two-dimensional fit. The methods were evaluated for their ability to detect the presence of motion, localize the camera angle at which motion occurred and measure the distance of motion. Patient motion was simulated by shifting motion-free images and then masking their periphery so that the field of view did not move on the image matrix. None of the methods detected 3.25 mm of motion with clinically useful accuracies. Visual inspection, cross-correlation and two-dimensional fit most accurately detected axial patient motion ($p < 0.05$), whereas cross-correlation most accurately detected lateral motion ($p < 0.05$). For axial motion, cross-correlation and two-dimensional fit most accurately localized the camera angle at which patient motion occurred ($p < 0.05$). For lateral motion, cross-correlation most accurately localized patient motion ($p < 0.05$). Two-dimensional fit measured the distance of axial patient motion to ± 1.1 mm and measured the distance of lateral motion to ± 8.7 mm. All other methods frequently overestimated or underestimated the distance of motion by > 13 mm. We conclude that cross-correlation adequately screens tomographic myocardial perfusion studies for both axial and lateral patient motion, although visual inspection is adequate for detection of axial motion. Cross-correlation best localizes the camera angle at which the motion occurred. Two-dimensional fit is the only method studied that accurately measures the distance of motion.

J Nucl Med 1993; 34:1341-1348

The evaluation of coronary artery disease using tomographic myocardial perfusion imaging (1,2) requires strict attention to quality control and recognition of imaging artifacts (3). One important quality control problem is patient movement during image acquisition (3-5). Patient movement may cause visual and quantitative artifacts in the reconstructed images (5-8) and motion artifact must be recognized to maintain diagnostic accuracy.

Several methods exist for detecting patient motion during tomographic myocardial perfusion imaging (4,9,10).

Received Nov. 12, 1992; revision accepted Mar. 18, 1993.
For correspondence and reprints contact: Jeffrey A. Cooper, MD, Nuclear Medicine, A-72, 47 Scotland Ave., Albany Medical Center, Albany, NY 12208.

Qualitative methods, such as visual inspection of a cine-graphic display of the raw data, are simple to implement and can alert the reader to the potential of image artifacts, but do not localize the camera angle at which motion occurred or measure the distance of motion. Quantitative methods estimate the distance of motion, the direction of motion and the camera angle at which the motion occurred. Quantitative methods can predict the incidence and location of image artifacts (7,8) and can be used for motion correction (5,10). To be suitable for these purposes, a motion correction method must accurately detect patient motion, correctly localize the camera angle at which motion occurred and correctly measure the distance of motion. To date, no one has comprehensively evaluated or compared the available methods for their accuracy in detecting, localizing or quantitating patient motion.

The purpose of this investigation was to compare the efficacy of the following methods of detecting patient motion: visual inspection of a rotating cinegraphic display, cross-correlation (9), diverging squares (10) and two-dimensional fit, a new method described in this paper. We measured the accuracy of all four methods for detecting motion. We also measured the accuracy of the automated methods for localizing the camera angle at which motion occurred and measuring the distance of motion.

METHODS

Visual Detection of Patient Motion

For the visual detection of patient motion, the observer viewed the raw data in a cinegraphic display on a 256 gray scale monochrome monitor. The observer could adjust the window and level of the gray scale, modify the cine framing rate, select between normal and inverted gray scales and adjust the position of a horizontal marker. At the observer's option, the images could be displayed in alternating forward and reverse sequence so that the patient appeared to rotate alternately from left to right and right to left. This prevented a jump between the first and last image in the cine sequence. The observer could also stop the cine and single step in either the forward or reverse directions. Abrupt motion was detected by observing a discontinuity in the motion of the heart between two successive images.

Cross-Correlation Method for Detection of Patient Motion

We used the cross-correlation method as previously described without modification (9). The cross-correlation function estimates the distance shifted between successive planar images. By

correcting these distances for gradual changes throughout the study, including the expected lateral interframe shift due to camera rotation, the program measures the distance of abrupt patient movement between frames. The program outputs the distance of interframe patient movement at each camera angle for both the axial and lateral axes.

Diverging Squares Method for Detection of Patient Motion

We used the diverging squares method as previously described without modification (10). This method estimates the coordinates of the heart center in each image. The program outputs the axial and lateral deviation of the heart center from its expected position as a function of camera angle.

Two-Dimensional Fit Method for Detection of Patient Movement

We developed the two-dimensional fit method to detect and quantitate patient motion during tomographic myocardial perfusion imaging. In the 45° image (left anterior oblique), the operator selects the center and radius of a circular region of interest (ROI) so that the circle clearly includes all of the myocardial counts. The pixels in this circle are compared to the adjacent image with the following equation:

$$SSE_{i,j} = \sum_k \sum_l (I_{x-k,y-l} - I'_{x-k,y-l})^2, \quad \text{Eq. 1}$$

where (x, y) is the coordinate of the center of the circular ROI, (k, l) ranges over the pixels of the circular ROI, I is the initial image and I' is the adjacent image. The minimum value of $SSE_{i,j}$ is found by parabolic interpolation. The coordinate of this minimum $(\Delta x, \Delta y)$ is the shift between the two images. The center of the circular ROI is placed over the adjacent image (I') at the coordinate $(x + \Delta x, y + \Delta y)$. This region is used to compare the next pair of adjacent images. The process repeats until all pairs of adjacent images are compared.

The horizontal coordinate of the center of the circular ROI in the left lateral planar image (90°) is used as the y position of the heart in transaxial plane. If the patient does not rotate about the axis of rotation, the y position of the heart in the transaxial plane will be constant at all camera angles since the patient is confined to the horizontal plane of the imaging table. The horizontal coordinate of the center of the circular ROI in the anterior planar image (0°) is used as the x position of the heart in the transaxial plane. By using the camera's center of rotation and the x and y positions of the heart in the transaxial plane during the 0° image, the expected lateral shift of the heart between successive projected images is calculated for each camera angle. The expected vertical interframe shift is 0 mm. The output of the program gives the axial and lateral deviations of the heart center from its expected position as a function of camera angle.

Study Database

The database consisted of motion-free postexercise ^{201}Tl SPECT studies performed on patients referred for evaluation of myocardial perfusion as described previously (7). Patients underwent treadmill exercise stress tests and were injected with 3 mCi of ^{201}Tl -chloride. The images were acquired on a General Electric 400AC gamma camera (GE Medical Systems, Milwaukee, WI) with a high-resolution, low-energy collimator and consisted of 32 40-sec 64×64 images over a 180° arc from 45° right anterior oblique to 45° left posterior oblique. Redistribution images were obtained 3–4 hr poststress. Patients were not reinjected with

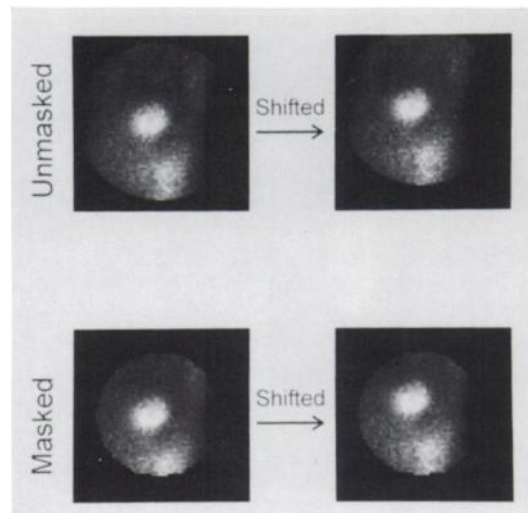


FIGURE 1. Effect of image masking on simulation of patient movement by image shifting. The top pair of images are unmasked and the entire field of view moves on the image matrix. The bottom pair of images are masked and the image moves through a smaller, but fixed field of view. For illustrative purposes, the figure shows a much larger distance of simulated motion and a much smaller radius of masking than used in the present study.

^{201}Tl -chloride before the redistribution images. Studies had to be motion-free to be included. Studies were considered motion-free if there was less than 3.25 mm (0.5 pixels) of movement by the cross-correlation method (9), no detectable movement on both visual inspection of a rotating cinegraphic display and on summed images and no streaking or smudging on reconstructed images. In contrast to previous studies (7), an equal number of poststress and redistribution images were used and both normal studies and studies with perfusion defects were used. One-third of the studies had perfusion defects.

Simulation of Patient Motion

Movement was simulated by shifting the planar images. Axial movement (along the length of the exam table) was simulated by shifting the images vertically. Lateral movement (along the width of the exam table) was simulated by shifting the images horizontally according to the formula: $d_i = d_T \cdot \cos(\phi_i)$, where d_i is the horizontal distance to shift image i , d_T is the distance of patient movement being simulated and ϕ_i is the angle of the camera to the patient for image i with 0° corresponding to the anterior image. The shifting was divided proportionately between the images before and after the point of movement to minimize translation of the reconstructed image. For example, 6.5 mm of upward movement at 22.5° (the eighth image) was obtained by shifting the first eight images down 4.9 mm and the last 24 images up 1.6 mm. Linear interpolation was used to simulate fractional pixel shifts. All of the images of control datasets were shifted by a nonintegral amount to control for the filtering effects of fractional shifts.

In both shifted and control images, pixels that were near the edge of the field of view were masked by setting them to zero, simulating a slightly smaller camera field of view. A circular mask was used with a radius equal to the field of view minus the distance of motion being simulated. Without masking (Fig. 1, top) the entire field of view appears to move on a fixed image matrix, which results in an inaccurate simulation of patient motion. Without masking, there is a strong bias toward increased detectability of motion. For example, an observer may detect small movements of the edge of the field of view before detecting movement

of the patient in a fixed field of view. In addition, some automated methods such as the cross-correlation method, can measure the distance movement of shifted, nonmasked images with a high degree of accuracy (9). With masking, the image appears to move within a fixed camera field of view (Fig. 1, bottom). When patients move, they also move within a fixed field of view. Therefore, image masking is required to accurately simulate the appearance of patient movement.

Accuracy of Visual Inspection for Detecting Patient Motion

We used receiver-operator characteristic curve analysis to measure the accuracy of visual inspection of a cinegraphic display of raw tomographic data to detect patient motion. Datasets were randomized equally among those containing: (1) simulated motion in one direction, (2) simulated motion in the opposite direction and (3) no motion. Datasets were then randomized equally among the following angles: -22.5° , 0° , 22.5° , 45° , 67.5° , 90° or 112.5° . If the dataset was randomized to contain simulated motion, the motion occurred at these angles. If the dataset was randomized to the control group, the dataset was assigned as a control for this angle. The observer viewed the dataset on the cinegraphic display described above. The observer knew the distance being simulated and whether the motion was axial or lateral, but was blinded to the angle of motion, the direction of motion (caudal versus rostral in axial motion or left versus right in lateral motion) and whether the image was a control image or contained motion. The images were scored on a point scale according to the certainty that it contained motion: (1) definitely no motion, (2) probably no motion, (3) uncertain, (4) probable motion and (5) definite motion. For each trial, the direction of movement was either axial or lateral and the distance of movement was constant. Testing trials were conducted for all combinations of 3.25 mm, 6.5 mm, 13 mm and 19.5 mm of movement (0.5, 1.0, 2.0 and 3.0 pixels, respectively) in the axial and lateral directions. Each trial tested 630 datasets with 90 datasets for each angle. At each angle there were 30 studies with motion in one direction, 30 studies with motion in the opposite direction and 30 control motion-free studies.

The diagnostic accuracy of the visual detection of patient movement was calculated by receiver-operating characteristic curve analysis using the computer program ROCFIT (11). The area under the ROC curve (z score or A_z) was interpreted as the accuracy for detecting patient motion when the prevalence of patient movement was 50% (12). An accuracy significantly greater than 50% at the 0.05 probability level by Student's t-test was considered to indicate detectable movement.

Evaluation of Automated Detection of Patient Movement

Control datasets and datasets with simulated motion were input to the cross-correlation, diverging squares and two-dimensional fit programs. The output of each program included: (1) the maximum interframe movement in the axial direction, (2) the camera angle at which the maximum interframe axial movement occurred, (3) the maximum interframe movement beyond expected in the lateral direction and (4) the camera angle at which the maximum interframe lateral movement occurred. The maximum interframe movement in the axial direction was considered to represent the distance of axial patient motion. The maximum interframe movement divided by the cosine of the camera angle was considered the estimated distance of lateral patient movement in a study. The camera angles with the maximum axial and lateral interframe

shifts were registered as the camera angles containing axial and lateral motion, respectively. Trials were conducted for all combinations of 3.25 mm, 6.5 mm, 13 mm and 19.5 mm of movement in the axial and lateral directions occurring at camera angles of -22.5° , 0° , 22.5° , 45° , 67.5° , 90° and 112.5° . Each trial tested 90 datasets. At each angle, there were 30 studies with motion in one direction, 30 studies with motion in the opposite direction and 30 control motion-free studies.

The diagnostic accuracy of detecting patient movement was calculated by receiver-operating characteristic curve analysis using the computer program LABROC (11). The value for the maximum interframe shift for the axial and lateral directions was used as the diagnostic index of the presence of motion. The area under the ROC curve (z score or A_z) was interpreted as the accuracy for detecting patient motion when the prevalence of patient movement was 50% (12). An accuracy significantly greater than 50% at the 0.05 probability level by Student's t-test was considered to indicate detectable movement.

Simulated motion was correctly localized when the camera angle predicted by the program to have movement was the same as the camera angle with simulated motion. The percentages of studies in which simulated motion was correctly localized and the standard deviations of these percentages were calculated (13). The significance of differences among percentages was evaluated by analysis of variance, and where appropriate, Student's t-test. The significance of differences between distributions was evaluated by chi-square.

Diagnostic precision was calculated from the mean value (\pm s.d.) of the measured maximal interframe shift as a function of the simulated distance of motion. The significance of differences among means was evaluated by analysis of variance, and where appropriate, Student's t-test.

RESULTS

When applied to the control (motion-free) datasets, the two-dimensional fit method measured a distance of motion of 2.9 ± 0.3 mm (mean \pm s.d.) in the axial direction and 3.6 ± 0.2 mm in the lateral direction. If the operator placed a larger circle over the heart or used a circle that was not centered on the heart, there was a $\pm 1.7\%$ variation in the measured distance, as long as the myocardial counts were within the initial circle. Using a larger circle increased the execution time of the program. Thus, the two-dimensional fit program is operator independent.

The diagnostic accuracy (\pm s.d.) of detecting patient motion as a function of the distance and direction of motion is shown in Figure 2A for axial motion and Figure 2B for lateral motion. All values shown were different from 50% accuracy ($p < 0.05$), except diverging squares at 3.25 mm of axial motion, diverging squares at 3.25 and 6.5 mm of lateral motion and visual inspection at 3.25 mm of lateral motion. For axial motion, there was no difference among visual inspection, two-dimensional fit and cross-correlation. For lateral motion, cross-correlation was the most accurate in detecting patient motion at distances of 3.25, 6.5 and 13 mm ($p < 0.05$). There was no difference between the accuracies of detecting motion in poststress versus delayed images. There was no difference between the accuracies of detecting motion in normal versus abnormal

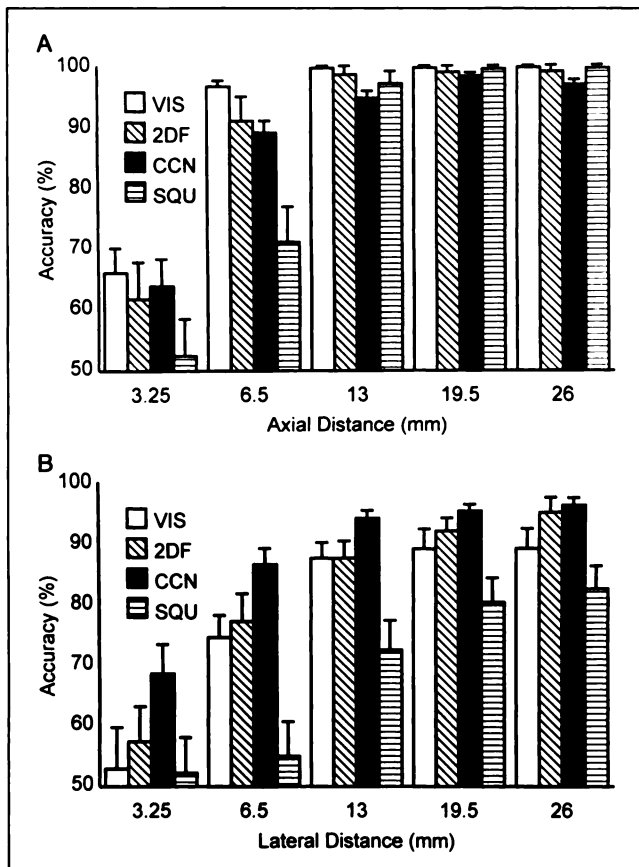


FIGURE 2. (A) The accuracy (\pm s.d.) of detecting axial patient motion by visual inspection of a rotating cinegraphic display (VIS), two-dimensional fit (2DF), cross-correlation (CCN) and diverging squares (SQU). The effect of distance and direction of motion is shown. (B) The accuracy (\pm s.d.) of detecting lateral patient motion by visual inspection of a rotating cinegraphic display (VIS), two-dimensional fit (2DF), cross-correlation (CCN) and diverging squares (SQU). The effect of distance and direction of motion is shown.

studies. For axial motion, there were no differences in the accuracy of detecting motion among camera angles (Fig. 3A). For lateral motion, there was worsening accuracy ($p < 0.01$) as the camera angle at the time of the motion approached the lateral (90°) projection (Fig. 3B).

The accuracy (mean \pm s.d.) of localizing the camera angle at which patient motion occurs is shown in Figure 4A for axial motion and Figure 4B for lateral motion. Among the three automated methods, the cross-correlation and two-dimensional fit methods most accurately localized the camera angle containing motion ($p < 0.05$). For lateral motion, cross-correlation was the most accurate at distances of 3.25 mm, 6.5 mm and 13 mm ($p < 0.05$). There was no difference in the accuracies of localizing motion in poststress versus delayed images or in normal versus abnormal studies. For axial motion, there were no differences among camera angles (Fig. 5A). For lateral motion, there were worsening accuracies ($p < 0.01$) as the camera angle approached the lateral (90°) projection at the time of the motion (Fig. 5B).

The accuracy and precision of measuring the distance of

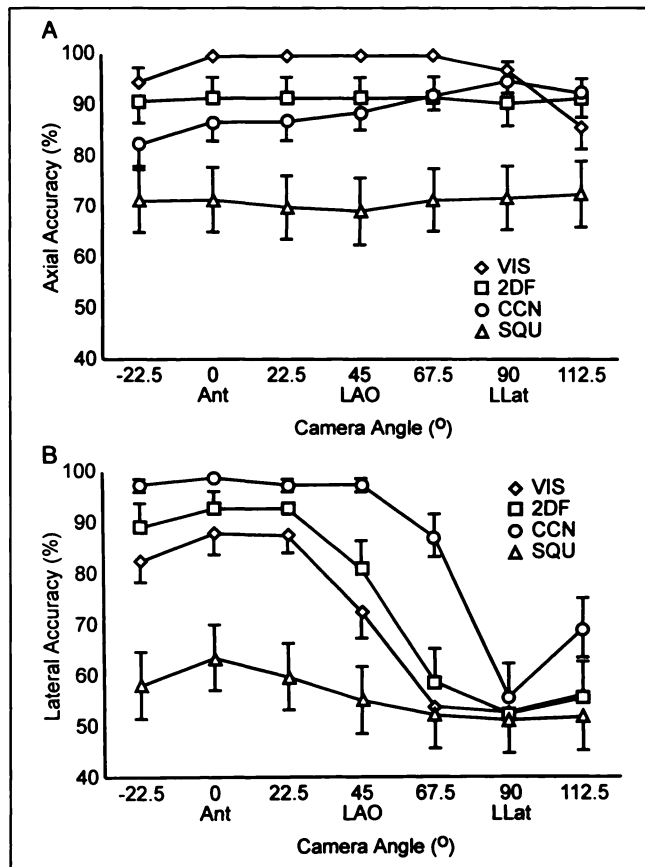


FIGURE 3. (A) The accuracy (\pm s.d.) of detecting 6.5 mm of axial patient motion by visual inspection of a rotating cinegraphic display (VIS), two-dimensional fit (2DF), cross-correlation (CCN) and diverging squares (SQU). The effect of the camera angle at which motion occurs is shown. (B) The accuracy (\pm s.d.) of detecting 6.5 mm of lateral patient motion by visual inspection of a rotating cinegraphic display (VIS), two-dimensional fit (2DF), cross-correlation (CCN) and diverging squares (SQU). The effect of the camera angle at which motion occurs is shown.

patient motion is shown in Figure 6A for axial motion and Figure 6B for lateral motion. Data shown are the measured distance of motion (mean \pm s.d.) as a function of the actual distance of motion. The dotted line is the line of identity. Among the three automated methods, the two-dimensional fit method most accurately measured the distance of patient motion ($p < 0.01$) with a precision of ± 2.6 mm for axial motion and ± 17.1 mm for lateral motion (95% confidence intervals). There was no difference between the accuracy of measuring the distance of motion between post-stress and delayed images or between normal and abnormal studies. For axial motion, there were no differences among camera angles (Fig. 7A). For lateral motion, there was worsening accuracy and precision ($p < 0.01$) as the camera angle at the time of the motion approached the lateral (90°) projection (Fig. 7B).

DISCUSSION

Methods for detecting patient motion can alert the reader to the potential presence of motion artifact in reconstructed images. For this purpose, a program that accu-

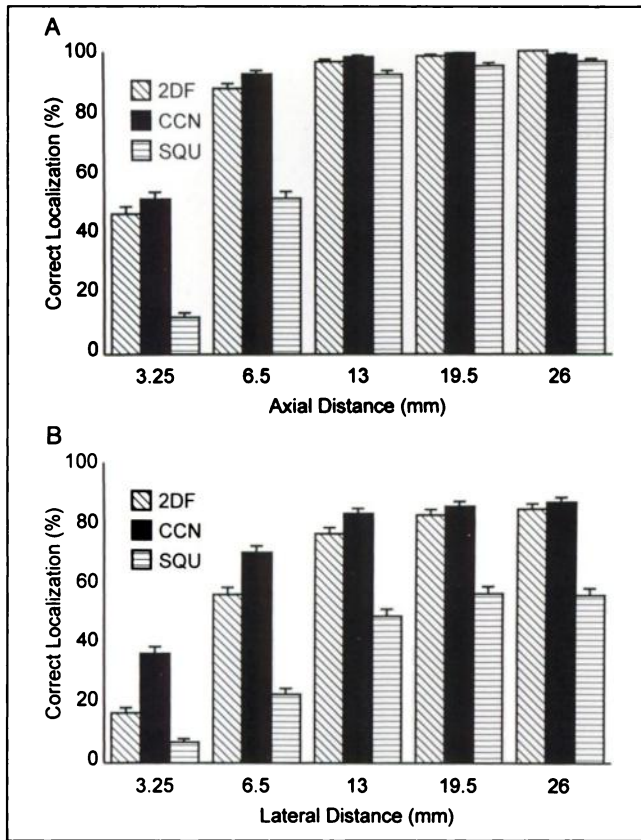


FIGURE 4. (A) The accuracy (\pm s.d.) of localizing the camera angle at which axial patient motion occurred by two-dimensional fit (2DF), cross-correlation (CCN) and diverging squares (SQU). The effect of the distance and direction of motion is shown. (B) The accuracy (\pm s.d.) of localizing the camera angle at which lateral patient motion occurred by two-dimensional fit (2DF), cross-correlation (CCN) and diverging squares (SQU). The effect of the distance and direction of motion is shown.

rately detects the presence of motion is sufficient. However, the incidence and anatomic location of artifacts depend on the distance, direction and timing of the movement (7,8). Therefore, quantitative motion detection methods that localize the camera angle at which motion occurred and measure the distance of motion can inform the reader of the likelihood of motion artifact in a particular vascular distribution. Quantitative motion detection can also provide the information needed by a motion correction algorithm to shift the moved images back to an unmoved position. For motion correction, the motion detection method must accurately detect, localize and measure patient motion.

In the current study, we evaluated the efficacy of four methods for detecting patient motion: visual inspection of a rotating cinegraphic display, cross-correlation (9), diverging squares (10) and two-dimensional fit, described in this paper. We evaluated the accuracy of detecting the presence of motion, the accuracy of localizing the camera angle at which motion occurred and the accuracy and precision of measuring the distance of motion.

Visual inspection, two-dimensional fit and cross-corre-

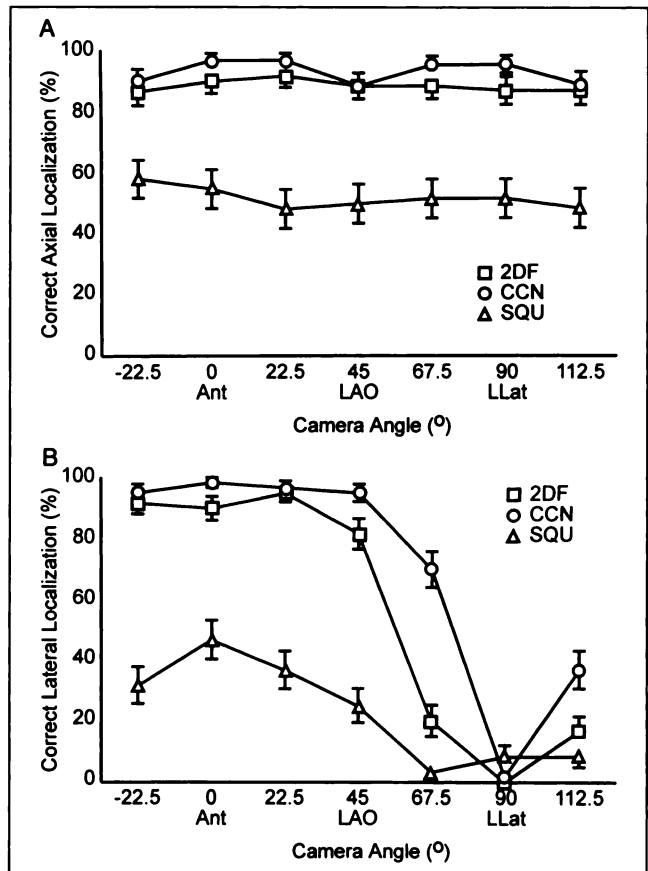


FIGURE 5. (A) The accuracy (\pm s.d.) of localizing the camera angle at which 6.5 mm axial patient motion occurred by two-dimensional fit (2DF), cross-correlation (CCN) and diverging squares (SQU). The effect of the camera angle at which motion occurred is shown. (B) The accuracy (\pm s.d.) of localizing the camera angle at which 6.5 mm lateral patient motion occurred by two-dimensional fit (2DF), cross-correlation (CCN) and diverging squares (SQU). The effect of the camera angle at which motion occurred is shown.

lation demonstrated accuracies of $>91\%$ for detecting ≥ 6.5 mm of axial motion (Fig. 2A). Cross-correlation demonstrated accuracies of $>87\%$ for detecting ≥ 6.5 mm of lateral motion (Fig. 2B). With these accuracies, either visual inspection, two-dimensional fit or cross-correlation are clinically useful for localizing ≥ 6.5 mm of axial patient motion and cross-correlation is clinically useful for the localization of ≥ 6.5 mm of lateral patient motion. Although some methods could detect 3.25 mm of patient motion, none had an accuracy exceeding 69% (Figs. 2A and 2B). Thus all the methods examined are of limited clinical value for ≤ 3.25 mm of motion.

The data for visual detection of patient motion in the raw data (Figs. 2 and 3) can be contrasted with the visual detectability of patient motion artifact in reconstructed images (7,8). At a given distance, patient motion was more easily detected as an abrupt shift of the heart in the raw data (Fig. 2) than as an artifact in the reconstructed images (7,8). Also, the detectability of axial patient motion in the raw data was independent of camera angle (Fig. 3), whereas the detectability of motion artifact in recon-

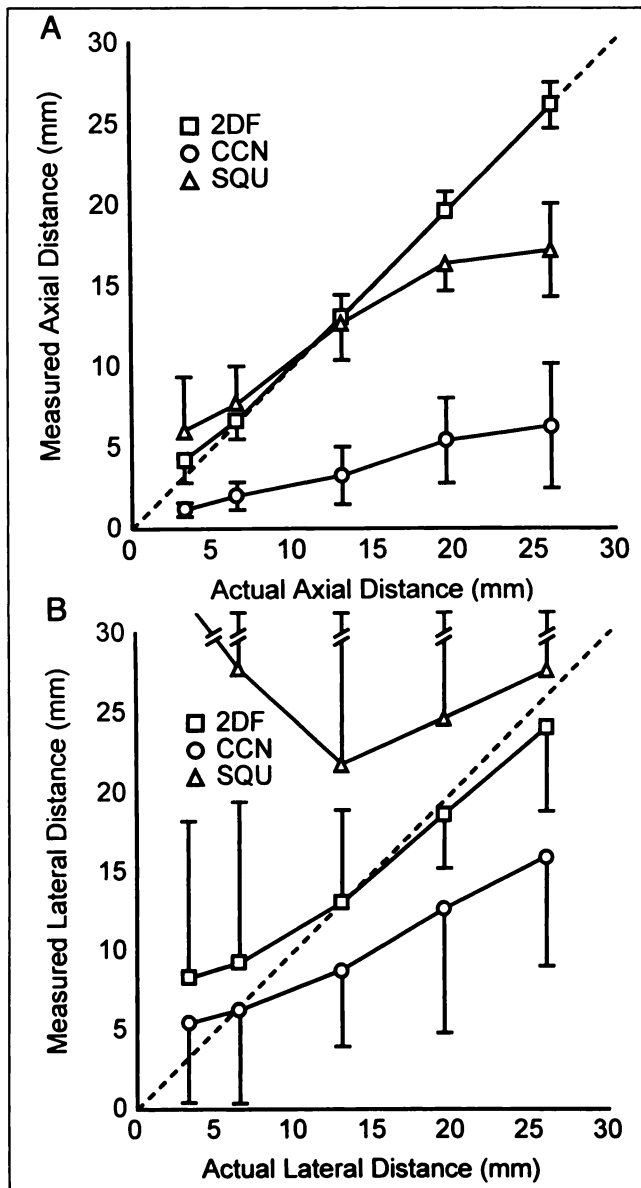


FIGURE 6. (A) The accuracy and precision of measuring patient motion by two-dimensional fit (2DF), cross-correlation (CCN) and diverging squares (SQU). The effect of the distance and direction of motion is shown. The dotted line shows the line of identity. Values are the mean \pm s.d. of the measured distance of motion. (B) The accuracy and precision of measuring patient motion by two-dimensional fit (2DF), cross-correlation (CCN) and diverging squares (SQU). The effect of the distance and direction of motion is shown. The dotted line shows the line of identity. Values are the mean \pm s.d. of the measured distance of motion.

structured images decreased at the beginning and end of the camera arc (7).

Both two-dimensional fit and cross-correlation localized motion with an accuracy $>88\%$ for ≥ 6.5 mm axial motion (Fig. 4A), and cross-correlation localized motion with an accuracy of $>83\%$ for ≥ 13 mm lateral motion (Fig. 4B). Thus, either two-dimensional fit or cross-correlation may be clinically useful to localize ≥ 6.5 mm axial patient motion and cross-correlation may be clinically useful to localize ≥ 13 mm lateral patient motion. Correct localization of

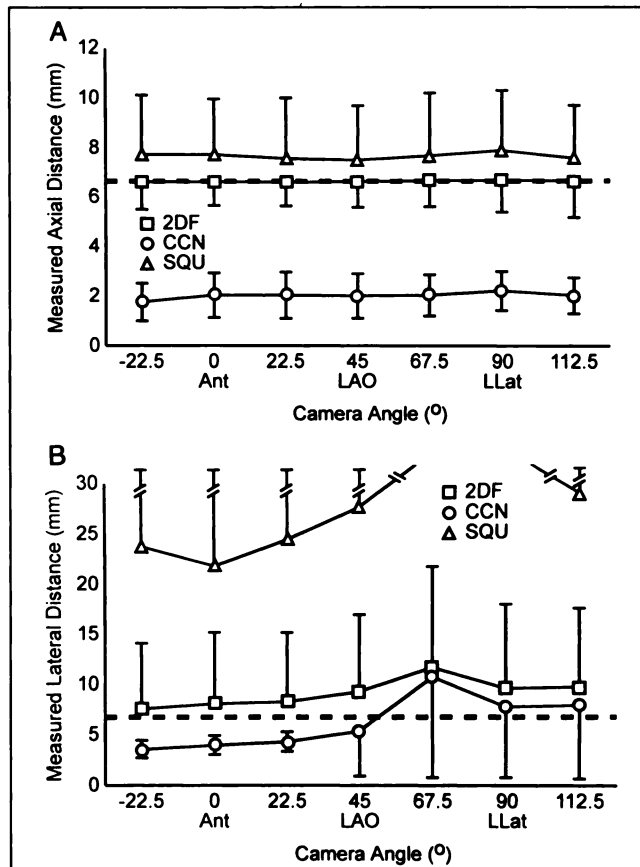


FIGURE 7. (A) The accuracy and precision of measuring 6.5 mm of axial patient motion by two-dimensional fit (2DF), cross-correlation (CCN) and diverging squares (SQU). The effect of the camera angle at which motion occurred is shown. The dotted line shows the distance of 6.5 mm. Values are the mean \pm s.d. of the measured distance of motion. (B) The accuracy and precision of measuring 6.5 mm of lateral patient motion by two-dimensional fit (2DF), cross-correlation (CCN) and diverging squares (SQU). The effect of the camera angle at which motion occurred is shown. The dotted line shows the distance of 6.5 mm. Values are the mean \pm s.d. of the measured distance of motion.

motion by these methods helps predict the effect of motion (7,8) and may be required for motion correction. None of the methods localized 3.25 mm of motion with a clinically usable accuracy (Figs. 4A and 4B).

The two-dimensional fit method was the most accurate and precise method for measuring the distance of patient motion (Fig. 6). Accurate knowledge of the distance of motion is required for predicting the effect of motion (7,8). It is likely that accurate knowledge of the distance of motion is also required for proper motion correction. Although the effect of >6.5 mm of motion is controversial (5,7,8,14), studies agree that clinically important artifacts will occur with 6.5 mm of axial movement and 13 mm of lateral movement (5,7,8). Therefore, if a motion correction method cannot shift the heart within 6.5 mm of its unmoved axial position and within 13 mm of its unmoved lateral position, residual motion artifacts will be expected even after motion correction. Both cross-correlation and diverging squares frequently underestimated or overesti-

mated the distance of motion by >13 mm (Fig. 6), and therefore are unsuitable for motion correction. Two-dimensional fit most accurately estimated the distance of motion, with a standard deviation of ± 1.1 mm for axial motion and a standard deviation of ± 8.7 mm for lateral motion. Motion correction based on the two-dimensional fit method would leave >3.25 mm of axial motion in $<0.5\%$ of studies but >13 mm of lateral motion in about 15% of studies. Thus, the measurement accuracy and precision of two-dimensional fit may be excellent for axial motion correction, even in situations in which 3.25 mm of motion causes artifacts (5,14) and passable for lateral motion correction.

Previous studies indicated that clinically important artifacts begin to occur with 6.5 mm of axial movement and 13 mm of lateral movement (7,8) although some investigators have found that 3.25 mm of motion will cause clinically important artifacts (5). The reason for this discrepancy is uncertain, but may be due to differences in equipment, processing or data analysis (14). If the clinical conditions allow 3.25 mm of motion to cause clinically important artifacts, this will be problematic as the methods evaluated in the current study could not accurately detect, localize or quantitate 3.25 mm of motion.

All methods detected, localized and measured axial motion more accurately than lateral motion (Figs. 2, 4 and 6). One explanation of this difference is the difficulty of detecting motion near the lateral camera angle (Figs. 3B, 5B and 7B) where the distance of motion projected onto the planar image is a small fraction of the actual distance. Another cause of this difference is the presence of baseline lateral motion. The heart's baseline lateral motion is proportional to its distance from the center of rotation and is dependent on the camera angle. The detection of lateral motion requires subtracting the heart's measured lateral position from its expected lateral position, a process that introduces more measurement error. Since there is no baseline axial motion, the detection of axial motion does not require subtraction of a baseline.

The cross-correlation method performed better than any other method in detecting and localizing lateral motion. A likely explanation of this finding is that the process of cross-correlation examines the entire image and becomes less accurate when the two images being correlated have increasing amounts of data unique to each image. Except in cases where the thorax is truncated, more counts move in and out of an image during axial movement than during lateral movement. Therefore, axially shifted image pairs have less data in common than laterally shifted image pairs. Sequential image pairs contain almost the same set of data. Thus, laterally moved image pairs can be more accurately correlated than axially moved pairs.

The diverging squares method, which measures motion in one-half pixel quanta (3.25 mm), detected motion poorly ≤ 13 mm. It detected 3.25 mm of motion in 55% of the control motion-free images and 6.5 mm of motion in 19% of the images. This is consistent with Poisson noise in making

quantized measurements. The diverging squares method also poorly localized and measured patient motion. Visual inspection of the program's output revealed that it worked well with many patient studies, but demonstrated two behaviors that contributed to its poor performance with other studies. First, the program occasionally tracked noncardiac structures. Second, large distances of abrupt motion were detected over two angles. For example, a 26-mm movement between 112.5° and 118.1° was detected as a 13-mm movement between 112.5° and 118.1° and a 13-mm movement between frames 118.1° and 123.8° . By our analysis, this was considered a 13-mm abrupt movement. The clinical utility of the diverging squares method may be improved by recognizing these problems.

Two important differences between the current studies and previous studies are the use of receiver-operator characteristic curve analysis and the use of image masking. Receiver-operator characteristic curve analysis allows an evaluation of diagnostic accuracy without assuming that a particular distance of movement is diagnostic of patient motion. This is important because each method detects a small amount of background movement, although the measured distance of motion may not be accurate.

Image masking after image shifting is critical for an accurate simulation of patient motion. Shifting the images without masking results in an inaccurate simulation of patient motion. To visualize this, imagine a rotating cinegraphic display of the raw data of a 32-angle thallium study. Now imagine that the last 16 images are shifted up by 2 pixels. The heart will move up two pixels between images 16 and 17, but so will the edge of the field of view (Fig. 1, top). In reality, patient motion does not cause the field of view to move on the image matrix. If the images are masked to a smaller radius that is fixed on the field of view, the heart will move up two pixels between images 16 and 17, but the edge of the field of view will remain fixed throughout the study (Fig. 1, bottom). Therefore, simulating patient motion by shifting images without masking the field of view represents an inaccurate simulation. For visual inspection, image masking prevents a reader from detecting patient motion solely by observing movement of the edge of the field of view on the image matrix. For automated methods, image masking requires the computer program to detect motion in a realistic simulation. For example, the cross-correlation method measures the distance of movement between shifted, nonmasked images with a high degree of accuracy (9), but in the present study had a reduced accuracy in a realistic simulation using shifted and masked images.

Correct receiver-operating characteristic curve analysis requires that the presence and absence of motion be certain. In these studies, the addition of simulated motion confirmed the presence of motion. The absence of motion was confirmed in part by the absence of motion artifact (streaking, blurring or beading) on reconstructed images. Using visual inspection and cross-correlation to verify the absence of motion reduced the likelihood of motion in the

control images, but may bias the results to higher accuracies for these methods.

Some types of patient motion were not evaluated in this study. Patients may rotate on the plane of the examining table or may rotate about the axis of camera rotation. All patients have some physiologic respiratory and cardiac motion and the respiratory movement may vary during a study and cause upward creep, a common source of motion artifact (15). In addition, combinations of translation and rotation or complex motion may occur that cannot be expressed with translation and rotation. We did not evaluate the effect of these types of motions on ^{201}Tl myocardial tomographic imaging.

Other visual methods exist for detecting patient motion that were not evaluated in this study. Detection of motion has been reported using inspection of summed images (4, 15) and inspection of the sinogram (3). Enhancement of the detection of motion using inspection of a rotating cinegraphic display has been reported by using radioactive point sources taped to the patient's chest (3, 4, 15). Both of these methods have been reported to be especially useful to distinguish patient motion from organ movement within the patient, as occurs with "upward creep" (15). Determination of the accuracy of these visual methods for detecting patient motion will require further studies.

In conclusion, high-quality SPECT myocardial perfusion imaging requires detection of patient motion. The presence of patient motion may be detected effectively by either visual inspection of a cinegraphic display of raw data, the cross-correlation method or the two-dimensional fit method. The development of better methods for motion correction will likely require algorithms that correctly localize the camera angle at which the motion occurred and accurately measure distance of motion. Cross-correlation

most accurately localizes the camera angle of motion but two-dimensional fit provides the most accurate and precise measurement of the distance of motion.

REFERENCES

1. Ritchie JL, Williams DL, Harp G, Stratton JL, Caldwell JH. Transaxial tomography with thallium-201 for detecting remote myocardial infarction: comparison with planar imaging. *Am J Cardiol* 1982;50:1236-1241.
2. Fintel DJ, Links JM, Brinker JA, Frank TL, Parker M, Becker LC. Improved diagnostic performance of exercise thallium-201 single photon emission computed tomography over planar imaging in the diagnosis of coronary artery disease: a receiver operating characteristic analysis. *J Am Coll Cardiol* 1989;13:600-612.
3. DePuey EG, Garcia EV. Optimal specificity of thallium-201 SPECT through recognition of imaging artifacts. *J Nucl Med* 1989;30:441-449.
4. Friedman J, Berman DS, Van Train K, et al. Patient motion in thallium-201 myocardial SPECT imaging: an easily identified frequent source of artifactual defect. *Clin Nucl Med* 1988;13:321-324.
5. Eisner R, Churchwell A, Noever T, et al. Quantitative analysis of the tomographic thallium-201 myocardial bull's eye display: critical role of correcting for patient motion. *J Nucl Med* 1988;29:91-97.
6. Zhu YY, Botvinick EH, O'Connell WJ, Dae MW. Tolerance of SPECT perfusion imaging to patient motion [Abstract]. *J Nucl Med* 1990;31:841.
7. Cooper JA, McCandless BK, Neumann PH. Effect of patient motion on tomographic myocardial perfusion imaging. *J Nucl Med* 1992;33:1556-1571.
8. Botvinick EH, Zhu YY, O'Connell WJ, Dae MW. A quantitative assessment of patient motion and its effect on myocardial perfusion studies. *J Nucl Med* 1993;34:303-310.
9. Eisner RL, Noever T, Nowak D, et al. Use of cross-correlation function to detect patient motion during SPECT imaging. *J Nucl Med* 1987;28:97-101.
10. Geckle WJ, Frank TL, Links JM, Becker LC. Correction for patient motion and organ movement in SPECT: application to exercise thallium-201 cardiac imaging. *J Nucl Med* 1988;29:441-450.
11. Metz CE. ROC methodology in radiologic imaging. *Invest Radiol* 1986;21:720-733.
12. Hanley JA, McNeil BJ. The meaning and use of the area under a receiver operating characteristic (ROC) curve. *Radiology* 1982;143:29-36.
13. Diamond GA. Limited assurances. *Am J Cardiol* 1989;63:99-100.
14. Eisner RL. Sensitivity of SPECT thallium-201 myocardial perfusion imaging to patient motion. *J Nucl Med* 1992;33:1571-1573.
15. Friedman J, Van Train K, Maddahi J, et al. "Upward creep" of the heart: a frequent source of false-positive reversible defects during thallium-201 stress-redistribution SPECT. *J Nucl Med* 1989;30:1718-1722.